Site-Specific Tryptophan Dynamics in Class A Amphipathic Helical Peptides at a Phospholipid Bilayer Interface

Andrew H. A. Clayton and William H. Sawyer
The Russell Grimwade School of Biochemistry and Molecular Biology, University of Melbourne, Parkville, 3052 Australia

ABSTRACT The amphipathic helix plays a key role in many membrane-associating peptides and proteins. The dynamics of helices on membrane surfaces might be of importance to their function. The fluorescence anisotropy decay of tryptophan is a sensitive indicator of local, segmental, and global dynamics within a peptide or protein. We describe the use of frequency domain dynamic depolarization measurements to determine the site-specific tryptophan dynamics of single tryptophan amphipathic peptides bound to a phospholipid surface. The five 18-residue peptides studied are based on a class A amphipathic peptide that is known to associate at the interface of phospholipid bilayers. The peptides contain a single tryptophan located at positions 2, 3, 7, 12, or 14 in the sequence. Association of the peptides with egg phosphatidylcholine vesicles results in complex behavior of both the tryptophan intensity decay and the anisotropy decay. The anisotropy decays were biphasic and were fitted to an associated model where each lifetime component in the intensity decay is associated with a particular rotational correlation time from the anisotropy decay. In contrast, an unassociated model where all components of the intensity decay share common rotational modes was unable to provide an adequate fit to the data. Two correlation times were resolved from the associated analysis: one whose contribution to the anisotropy decay was dependent on the exposure of the tryptophan to the aqueous phase, and the other whose contribution reflected the position of the tryptophan in the sequence. The results are compared with existing x-ray structural data and molecular dynamics simulations of membrane-incorporated peptides.

INTRODUCTION

A number of studies have revealed that water-soluble proteins undergo structural fluctuations that are believed to be important for biological function. Less information is known about structural fluctuations within membrane-associated proteins. The importance of the latter is evident when it is recognized that approximately 30 to 40% of the proteins coded in the human genome are associated with membranes.

Time-resolved fluorescence anisotropy studies of membrane proteins and peptides containing intrinsic or extrinsic fluorophores are capable of providing direct information on structural fluctuations occurring during the excited state lifetime of the fluorophore. In the case of membrane-incorporated polypeptides containing transmembrane helical segments, these studies have revealed the presence of local probe motions, segmental motions, and hindered helical fluctuations about an axis parallel to the membrane normal. A particularly interesting example is the work of Vogel and coworkers, who mapped the site-specific tryptophan motional dynamics at different sequence positions along the length of a transmembrane polypeptide (Vogel et al., 1988). The dynamics of the tryptophans was greater near the ends of the peptide rather than at the center, despite there being a microviscosity gradient in the lipid bilayer in the opposite direction. There have been no corresponding tryptophan mapping studies with peptides that contain α-helices aligned parallel to the lipid bilayer surface. The question of whether tryptophan motional dynamics in an amphipathic helix are correlated with the tryptophan position with respect to the aqueous or membrane phases has not been addressed. Here we report the dynamics of a set of 18-residue amphipathic α-helical peptides, each containing a single tryptophan at sequence positions 2, 3, 7, 12, or 14 (Fig. 1). Recent biophysical (Clayton and Sawyer, 1999a,b) and x-ray structural studies (Hristova et al., 1999) have indicated that these peptides associate with the interface of lipid bilayers to form α-helices that align predominantly parallel to the membrane surface. In this conformation the tryptophan at position 12 and near center of the polar face of the helix is located in a polar, aqueous-exposed environment. The tryptophans at positions 3, 7, and 14 (near the center of the nonpolar face of the helix) are in nonpolar, water-shielded environments, and the tryptophan located near the peptide polar-nonpolar interface at position 2 shows intermediate behavior. Time-resolved tryptophan fluorescence studies on the peptide-lipid complexes reveal the presence of two components attributed to two populations of tryptophan rotamers created via rotation of the indole ring about the tryptophan $C_\alpha - C_\beta$ bond (Clayton and Sawyer, 1999b). In the present work we extend these studies to examine the time-resolved fluorescence anisotropy of the single tryptophan residue of each peptide in unilamellar phospholipid vesicles using the frequency domain method.

Received for publication 12 November 1999 and in final form 16 May 2000.

A. H. A. Clayton's current address: Department of Molecular Biology, Max Planck Institute for Biophysical Chemistry, Gottingen, D-37077, Germany. E-mail: clayton@mpc186.mpibpc.gwdg.de.

Address reprint requests to A. H. A. Clayton and W. H. Sawyer, The Russell Grimwade School of Biochemistry and Molecular Biology, The University of Melbourne, Parkville, Australia 3052. Tel.: 61-3-9344-5923; Fax: 61-3-9347-7730; E-mail: w.sawyer@biochemistry.unimelb.edu.au.

0006-3495/00/08/1066/08 $2.00

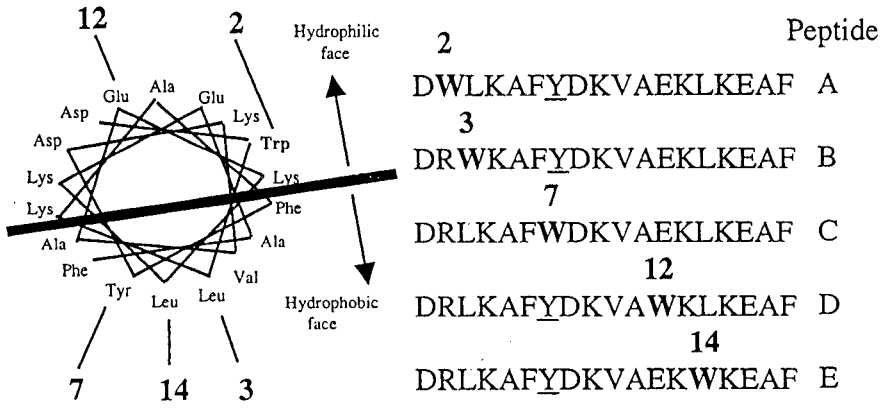

FIGURE 1 Helical wheel representation of 18-residue amphipathic peptides. The figures in bold refer to the positions of tryptophan substitution in peptides A-E. The *solid line* represents the putative boundary between the hydrophilic and hydrophobic faces of the α-helix.

The results are compared with existing models of amphipathic peptides at lipid surfaces.

MATERIALS AND METHODS

Materials

Egg yolk phosphatidylcholine was purchased from Lipid Products (Nutfield, UK). Peptides with the sequences listed in Fig. 1 were synthesized using automated solid-state synthesis in conjunction with Fmoc chemistry as described previously (Clayton and Sawyer, 1999a). Purification was by reverse phase high performance liquid chromatography, and the purity and identity of the peptides was checked by matrix-assisted laser desorption and ionization time-of-flight mass spectrometry (MALDI-TOF).

Methods

Small unilamellar vesicles were prepared by sonication of a suspension of egg yolk phosphatidylcholine in 10 mM Tris buffer, 150 mM NaCl, pH 7.4, as described by New (1990). Peptide-lipid complexes were prepared by addition of an aqueous suspension of vesicles to a solution containing a known concentration of peptide. The final concentrations of peptide and lipid were 20 μM and 4 mM, respectively, to give a lipid-to-peptide molar ratio of 200:1. Fluorescence intensity and anisotropy titrations showed that under these conditions, all the peptide was bound to the lipid surface (results not shown).

Fluorescence anisotropy decays were measured with a SPEX Fluorolog-τ2 frequency domain spectrofluorometer employing 10 to 20 frequencies in the range of 5 to 150 MHz. Excitation of tryptophan was accomplished using vertically polarized 295 nm excitation from a 1000W Hg-Xe lamp (Model 1909M Oriel, Stratford, CT). An emission polarizer was set to alternate between vertical or horizontal positions under computer control, and the corresponding phase angles and AC components of the tryptophan fluorescence were observed through a 320-nm cutoff filter. The data were fully corrected for polarization biases in the detection system. Intensity decays were collected as described previously (Clayton and Sawyer, 1999b), but observed through a 320-nm cutoff filter. The cell block was maintained at 20°C with a circulating water bath. Globals Unlimited Software (University of Illinois, Champaign-Urbana, IL) was used to fit the frequency domain data to an associative model in which each specific lifetime in the fluorescence intensity decay is linked to a specific rotational correlation time. An associative component having an infinite correlation time on the fluorescence time scale (10,000 ns), a short lifetime (0.05 ns), and a large limiting anisotropy (0.85) was included to account for vesicle scatter. Control experiments with sonicated egg phosphatidylcholine vesicles and zwitterionic tryptophan, which does not bind to vesicles (Ladokhin et al., 1997), showed that this analysis procedure is capable of describing the anisotropy decay of tryptophan in the presence of up to 60% background scatter. Full details of the analysis procedure will be presented in a future publication (Clayton, Klonis, and Sawyer, unpublished results). For the membrane-associated peptides, two lifetimes were required to fit the intensity decays; therefore, two associated correlation times were used in the fitting procedure. Another model was considered in which the rotational correlation times were common to the set of peptides and therefore linked in the analysis. The goodness of fit was determined by χ^2 analysis. A comparison of different fluorescence anisotropy decay models was made by inspection of a χ^2 ratio (χ^2_R) between the model under consideration and a defined model. For the individual free-float sum-of-exponentials decay analysis, the ratio χ^2_R was that between the free-float parameter model χ^2 and a single exponential decay model χ^2. To assess the penalty associated with linking parameters globally, the global-linked χ^2 for each peptide was divided by the best fit sum of exponential χ^2.

RESULTS

Time-resolved fluorescence anisotropy

The dynamic depolarization data for the peptide-vesicle complexes were fitted to a discrete associated decay model involving the sum of two exponential lifetime terms and two rotational correlation times.

$$r(t) = [r_1(t)A_1\exp(-t/\tau_1) + r_2(t)A_2\exp(-t/\tau_2)]/[A_1\exp(-t/\tau_1) + A_2\exp(-t/\tau_2)]$$

$$r_1(t) = r_{o1}\exp(-t/\phi_{11})$$

$$r_2(t) = r_{o2}\exp(-t/\phi_{22})$$

where τ_1 and τ_2 are the time constants, A_1 and A_2 are the corresponding pre-exponential population amplitudes of the fluorescence decay, $r_1(t)$ and $r_2(t)$ are the lifetime-associated anisotropy decays, ϕ_{11} and ϕ_{22} are the rotational correlation times, and r_{o1} and r_{o2} are the limiting anisotropies. In accord with published work, two time constants were determined from the intensity decay of each peptide-lipid complex: a major component of 2.5 ns and a minor component of 6.5 ns

(Clayton and Sawyer, 1999b). The short and long time constants were in the range reported previously but the pre-exponential amplitudes differed by ~10% from previous work (results not shown). The source of these small differences most likely lies in the different emission configurations used. A contribution due to vesicle scatter was also included in the fitting procedure, as outlined in Materials and Methods. In contrast, models involving unassociated correlation times (one or two), wherein all fluorescence lifetime components share the same anisotropy decay (Eq. 4), were unable to provide a satisfactory description of the data and produced values of χ^2_R that were over 100-fold greater than the associated two-correlation time model (Table 1).

$$r(t) = r_o[\alpha \exp(-t/\phi_\alpha) + \beta \exp(-t/\phi_\beta)]$$

where r_o is the zero time anisotropy for the tryptophan residue, α and β are fractional contributions, and ϕ_α and ϕ_β are the correlation times (Globals Unlimited Software).

The analysis of the peptide-lipid complexes was carried out in two stages. In the first stage the intensity decay parameters were fixed at the values obtained from separate intensity decay experiments but the parameters in the anisotropy decays were varied. A free-floating-parameter analysis of the anisotropy parameters revealed two rotational correlation times, a small correlation time in the range 0–3 ns and a large correlation time of 3–60 ns (Table 1) for the membrane-associated peptides. The floated zero-time anisotropies were in the range expected for tryptophan excited at 295 nm, i.e., $r_o < 0.24$ (Valeur and Weber, 1977). Two features are of particular note. First, with respect to ϕ_{11}, the negligible values measured for peptide A (tryptophan at position 2) and D (tryptophan at position 12) suggested that at these positions, the fluorescence associated with the short lifetime component is almost completely depolarized. Second, there is a gradual decrease of ϕ_{22} in peptides A-E while the r_{o2} values remain fairly constant, indicating a gradual sequence-dependent depolarization of the long lifetime component-associated fluorescence as the tryptophan is moved from position 2 to position 14.

We questioned whether the data could be analyzed in terms of an alternative model where the set of peptide-lipid complexes possessed a common set of rotational modes. Thus, in the second stage of fitting, the short and long correlation times were assumed to be common among the peptides and were therefore linked in the analysis, whereas the associated limiting anisotropy values were allowed to vary and were floated in the analysis. We note that this global approach (Knutson et al., 1983) reduces the number of variable parameters from 20 to 12 as compared to the free-float analysis for the set of five peptide-lipid complexes as a whole. A comparison of the χ^2 and the calculated anisotropy $\langle r \rangle$ between the two fitting procedures indicated that the assumption of common rotational correlation times provided an equivalent description of the dynamic depolarization for the peptide-lipid complexes. A typical global fit of the experimental data is presented in Fig. 2, and the results are summarized in Table 2. An additional consequence of using the global approach is that the derived correlation times are determined to better precision at the 67% confidence interval. A linked-correlation time analysis revealed two correlation times for the peptide-lipid complexes, a short correlation time of 2.5 ns (67% confidence interval 2.3–2.8 ns) and a long correlation time of 27 ns (67% confidence interval 21–37 ns). The short correlation time associated limiting anisotropy values (r_{o1}) fell into two groups: 0 (average 67% confidence interval −0.06 to 0.04) for peptides with tryptophans at positions 2 and 12, and 0.16–0.24 (67% confidence interval 0.13–0.24) for the peptides with the tryptophans at positions 3, 7, and 14. The limiting anisotropies (and 67% confidence intervals) associated with the long correlation time (r_{o2}) showed a gradual decrease from 0.21 (0.20–0.24) for the peptide with tryptophan at position 2 (peptide A), to 0 (0–0.01) for the peptide with the tryptophan at position 14 (peptide E). An alternative model employing common limiting anisotropy

TABLE 1 Lifetime-associated rotational correlation times (ϕ_i), apparent limiting aniostropies (r_{o1}), and steady-state anisotropies ($\langle r_i \rangle$) for 18-residue amphipathic peptides bound to unilamellar bilayer vesicles

	Rotational correlation time data						
Peptide*	ϕ_{11} (ns)	ϕ_{22} (ns)	r_{o1}	r_{o2}	$\langle r \rangle^\dagger$	$\chi^{2\ddagger}_R$ associated	$\chi^{2\S}_R$ unassociated
A(2)	<0.1	31.679	0.240	0.213	0.102	0.006	0.8
B(3)	1.181	11.685	0.143	0.240	0.109	0.002	0.8
C(7)	0.721	10.217	0.161	0.240	0.103	0.002	0.9
D(12)	<0.1	55.865	0.240	0.110	0.058	0.001	0.8
E(14)	2.535	1.585	0.187	0.159	0.065	0.001	0.7

*Position of the tryptophan residue in the peptide sequence indicated in parenthesis.

†Anisotropy $\langle r \rangle$ was calculated from time-resolved fluorescence parameters as:

$\langle r \rangle = \{[r_{o1}A_1\tau_1/(1 + (\tau_1/\phi_{11}))] + [r_{o2}A_2\tau_2/(1 + (\tau_2/\phi_{22}))]\}/(A_1\tau_1 + A_2\tau_2)$

‡Ratio of χ^2 of the associated two-correlation-time model to that of an unassociated single-correlation-time model.

§Ratio of χ^2 of the unassociated two-correlation-time model to that of the unassociated single-correlation-time model.

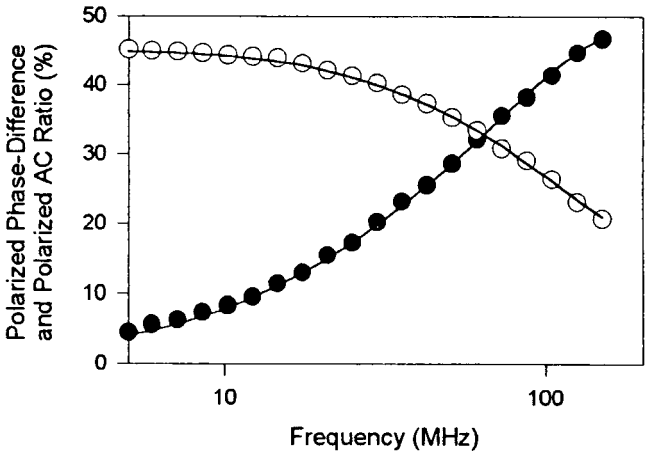

FIGURE 2 Anisotropy decay of the tryptophan fluorescence for peptide E complexed with egg phosphatidylcholine vesicles. The phase difference between the vertically polarized and horizontally polarized components of the emission is denoted by the *hollow circles* and the corresponding AC ratio is denoted by the *filled circles*. The *solid lines* represent the fits of the data carried out as described in Materials and Methods and reported in Table 2.

values but floated correlation times was also considered but produced poor fits ($\chi^2_R > 10$).

Data were also collected for the peptides in free solution (i.e., in the absence of lipid). In general, the anisotropy decays could be fitted to a single unassociated correlation time in the range from 0.5 to 1.5 ns. However, it is likely that the time scale of the rotamer motion and the global rotational motion overlaps in this region and cannot be resolved, and the analysis was not pursued.

DISCUSSION

Origin of the dynamic depolarization phenomenon

The observed decays of fluorescence anisotropy could result from two main sources: First, excited state decay of different rotationally frozen states, with each state possessing a unique and associated transition moment orientation, limiting anisotropy and fluorescence lifetime. Second, rotational dynamics of the indole fluorophore arising from structural fluctuations of the peptide on the lipid surface

The first effect can be discounted on the basis of two observations. First, rotationally frozen populations would be expected to yield a residual anisotropy at long times. This is not observed experimentally. Second, the decay of anisotropy would be affected by the limiting anisotropies, fluorescence lifetimes, and pre-exponential amplitudes (see Eq. 1). This would imply a correlation between the intensity decay and the anisotropy decay for the set of peptide-lipid complexes. This is not observed. Therefore, we conclude that the primary source of the anisotropy decays can be attributed to structural fluctuations of the peptide on the lipid surface. We now turn to a discussion of these structural fluctuations in more detail.

Assignment of rotational modes as structural fluctuations

According to the fluorescence dynamic depolarization measurements, at least two molecular motions of the tryptophan residue in the interface-associated polypeptides could be distinguished: 3 ns and 30 ns (Table 2). In addition, unresolved processes were also evident from the observation of limiting anisotropies that were smaller than expected for an immobilized tryptophan residue ($r_o = 0.22–0.24$ exciting at 295 nm; Valeur and Weber, 1977). Several lines of evidence suggest that the short (3 ns) correlation time is associated with local fluctuations of the indole ring with respect to the polypeptide main chain. Previous studies of tryptophan anisotropy decay in membrane proteins have correlated subnanosecond-nanosecond motions with local indole fluctuations (Dornmair and Jahnig, 1989; Vogel et al., 1988; Maliwal et al., 1986). The depolarization of tryptophan fluorescence associated with the short lifetime component is also correlated with the exposure of the tryptophan residue to the aqueous phase. Thus, the tryptophan at position 12 (Peptide D), which we have shown previously resides in an aqueous environment (Clayton and Sawyer, 1999a), exhibits fluorescence associated with the short lifetime component that is the most depolarized on the basis of a low r_{o1} value and low steady-state polarization ($\langle r \rangle$, Table 2). Conversely, tryptophans at positions 3, 7, and 14 are least exposed to the aqueous phase but their short lifetime component-associated fluorescence shows the largest anisotropy values of r_{o1} and $\langle r \rangle$.

The 30-ns correlation time may be assigned to a combination of helix fluctuations and rotational diffusion on the surface of the lipid bilayer. Two arguments may be presented to support this assignment. First, a value of 30 ns is in the range reported for helix fluctuations of other helical peptides in bilayer vesicles. For example, the single tryptophan in melittin (John and Jahnig, 1988; Maliwal et al., 1986) and in polypeptide analogues of alamethicin (Vogel et al., 1988; Doring et al., 1997) undergoes slow relaxation processes in the range from 10 to 50 ns. Second, the magnitude of the long correlation time is in agreement with theoretical estimates based on rotational precession of the helices on the lipid surface and/or hindered helix fluctuations. To obtain an order-of-magnitude estimate for the rotational correlation time, we consider two models based on rigid body rotational diffusion and rigid body fluctuations within an ordering potential. Considering the polypeptide helix as a cylinder of length 27 Å and diameter 10 Å the rotational diffusion coefficient associated with precession about the cylinder short axis (D_r) is given in terms of the length of the cylinder (L), the cylinder translational diffu-

TABLE 2 Lifetime-associated and globally-linked rotational correlation times (ϕ_l), apparent limiting anisotropies (r_{oi}), and steady-state anisotropies ($\langle r_i \rangle$) for 18-residue amphipathic peptides bound to unilamellar bilayer vesicles

	Global-linked Rotational Correlation Time Data					
Peptide*	ϕ_{11} (ns)	ϕ_{22} (ns)	r_{o1}	r_{o2}	$\langle r \rangle^{\dagger}$	χ^2_R
A(2)	2.545	27.903	0.000	0.217	0.102	1.0
B(3)	2.545	27.903	0.159	0.161	0.109	1.6
C(7)	2.545	27.903	0.170	0.146	0.105	1.7
D(12)	2.545	27.903	<0.03	0.119	0.057	1.0
E(14)	2.545	27.903	0.241	<0.01	0.065	1.0

The chi-squared ratio (χ^2R) is defined as the ratio of the chi-squared from the global fit to that of the chi-squared from an unlinked lifetime-associated fit. The parameters in Table 2 result from an analysis assuming common rotational modes among the set of five peptides (correlation times are linked for the set of peptides) and differ from that of Table 1.

*Position of the tryptophan residue in the peptide sequence indicated in parenthesis.

†Anisotropy $\langle r \rangle$ was calculated from time-resolved fluorescence parameters as:
$\langle r \rangle = \{[r_{o1}A_1\tau_1/(1 + (\tau_1/\phi_{11}))] + [r_{o2}A_2\tau_2/(1 + (\tau_2/\phi_{22}))]\}/(A_1\tau_1 + A_2\tau_2)$.

sion coefficient (D_L), and some constants which take into account end effects, as formulated in the model of Tirado et al. (1984), viz.:

$$D_r = 4D_L/(L^2)$$

We believe the present formulation in terms of the lateral diffusion coefficient is physically reasonable for the case of a surface-associating peptide, because peptide rotational precession and peptide lateral diffusion involve transfer of matter along the same plane, i.e., the membrane surface. We have no experimental measurement of D_L for the present peptides. However, a value for D_L of 8×10^{-8} cm^2 s^{-1} has been measured for a surface-associated 25-residue peptide on fluid hydrated 1-palmitoyl 2-oleoyl phosphatidylcholine multilayers (Frey and Tamm, 1990). Using this value for D_L and the cylinder length given above, a value for D_R of 4×10^6 s^{-1} is obtained. If it is assumed that the absorption or emission moments of the indole ring are fixed parallel to the cylinder axis, the rotational correlation time associated with cylinder precession is given by $1/(6D_R)$, corresponding to a value of 42 ns. Another possibility is that the long correlation time represents hindered motion of the helix on the membrane surface. In this case the correlation time for rotational diffusion in the limit of highly hindered motion is given by

$$\phi = \langle \nu^2 \rangle / 2D_r$$

(Dornmair and Jahnig, 1989). Here, $\langle \nu^2 \rangle$ denotes the mean square fluctuations about an angle ν between the long axis of the helix and its mean orientation, and D_r denotes the coefficient for rotational diffusion about the helix short axis, as discussed above. The value of the mean-squared fluctuation of the helix can be estimated from recent oriented circular dichroism measurements (Clayton and Sawyer, 2000) which show that the helical peptide 18A has an order parameter of -0.30 in hydrated fluid-phase dimyristoyl phosphatidylcholine multilayers (Fig. 3), corresponding to an effective fluctuation of $\langle \nu^2 \rangle = 0.27$ radians about an axis parallel to the membrane surface. Using these results, we obtain a correlation time value corresponding to hindered whole body fluctuations of the order of 34 ns. It is noted that although both models presented above are in reasonable agreement with the experimental data, they are presented only for the purpose of gaining a crude estimate of the expected correlation time. Many molecular details of the peptide and membrane are neglected in these models that would be required in a more sophisticated theoretical treatment of the polypeptide dynamics. For example, we have not taken into account the possibility of rigid body rotation of the helix about its long axis. As will be discussed later, rotation of the peptide about its long axis on the lipid surface would be energetically unfavorable and, if it oc-

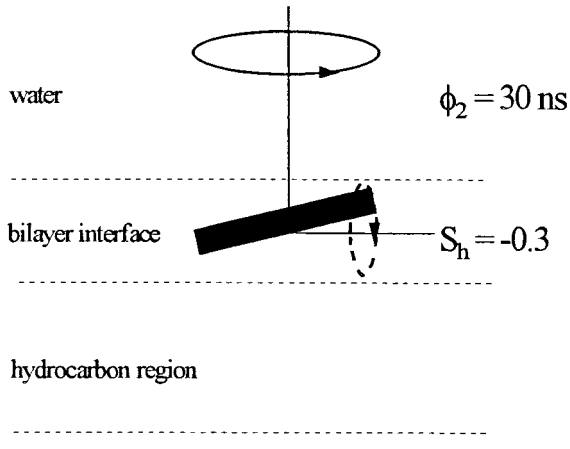

FIGURE 3 Interpretation of helix dynamics on the membrane surface incorporating a combination of helix precession and tilting motions. The experimentally determined long relaxation time is shown ($\phi_{22} = 30$ ns) and corresponds closely to that calculated from theory (see Eqs. 4 and 5). The helix orientation order parameter of peptide A in fluid dimyristoyl phosphatidylcholine multilayers ($S_h = -0.3$) was taken from oriented circular dichroism experiments of peptide A in fluid hydrated dimyristoylphosphatidylcholine multilayers (Clayton and Sawyer, 2000).

curred, would be severely hindered. A rigid cylinder model of rotational diffusion also neglects fluorophore depolarization processes due to segmental fluctuations and local motions of the fluorophore about its point of attachment to the macromolecule.

The question now arises as to the origin of the associated anisotropy decays in the present systems. Associated anisotropy decays have been reported previously in protein-lipid systems. Peng and coworkers (1990) attributed the anomalous anisotropy decay of the single tryptophan of bacteriophage M13 coat protein associated with lipid vesicles to the location of the tryptophan residue in two different sites differing in fluorescence lifetime, anisotropy, and orientation with respect to the protein and lipid environments. The relationship between tryptophan environment and tryptophan dynamics is further exemplified by molecular dynamics simulations of aromatic residues in protein-lipid complexes. In one such study it was found that exposed aromatic ring conformations underwent rapid relaxation processes, whereas conformers in close contact with the polypeptide main chain were less mobile and exhibited more restricted motion on the simulation time scale (Tieleman et al., 1998). The distance between the indole ring and quenching groups in the polypeptide and external medium is also an important determinant of excited state lifetime and suggests that an association between conformer lifetime and associated anisotropy might be predicted. Indeed, one prediction of the rotamer model of tryptophan photophysics (Chen et al., 1991; Szabo and Rayner, 1980) is that two or more indole rotamers are populated but do not interconvert on the fluorescence time scale, implying distinct lifetimes and associated anisotropies. X-ray surveys of tryptophan rotamer distributions in peptides also point to the possibility of tryptophan rotamer-dependent dynamics. Inspection of joint χ-1;χ-2 distributions (reflecting indole rotations about the C_α—C_β and C_β—C_γ bonds, respectively) from x-ray crystallographic surveys of peptides show that tryptophan χ-1 rotamers that are farthest from the polypeptide main chain populate a wider range of χ-2 angles than χ-1 rotamers, which are more proximal to the peptide main chain (Benedetti et al., 1983). This suggests that steric constraints imposed by the polypeptide main chain might result in χ-1 rotamer-dependent dynamics, and by inference, associated anisotropy decays. Furthermore, tryptophan conformers or rotamers that differ in the orientation of the absorption/emission transition moments with respect to the main chain may preferentially sense different anisotropic motional forms. This is expected on the basis of theory (Belford et al., 1972) and has been observed experimentally (Beechem et al., 1986) for various protein-dye conjugates.

The aforementioned considerations are in accord with our results on the present peptide-lipid systems. The differences in the magnitude of the two correlation times and in their relative dependence/independence on tryptophan micropolarity and associated lifetime are consistent with the tryptophan residue being located in (at least) two distinct environments differing in exposure of the tryptophan to the polypeptide main chain and solvent. We previously attributed the lifetime heterogeneity in the intensity decays to tryptophan rotamers created via rotation of the indole ring about the $C_\alpha-C_\beta$ bond. The present results add to our previous data and provide additional evidence for this model. In terms of the rotamer model, the short lifetime/short correlation time fluorescence originates from a solvent-exposed tryptophan conformer/rotamer, whereas the corresponding associated long lifetime/long correlation time component represents a tryptophan conformer that is in closer contact with the polypeptide main chain and reorients as a result of main chain segmental fluctuations and rotational diffusion. An alternative model proposes a distribution of environments and/or rotational correlation times (Alcala et al., 1987; Alcala, 1995). In this case the discrete lifetime and rotational correlation times presented in Tables 1 and 2 would represent the approximate modes of the distribution in question (Peng et al., 1990). Although the photophysics of tryptophan-containing peptides and indole derivatives are extremely complex (Millar 1996), and in particular may involve contributions from solvent dipolar relaxation effects (Ladokhin, 1999), the total fluorescence and anisotropy decays of the amphipathic peptides discussed here and previously (Clayton and Sawyer, 1999a,b) are consistent with lifetime-associated anisotropy decays and the rotomer model of tryptophan dynamics.

Comparison with x-ray data for class A amphipathic helices in lipid multilayers

The results of the site-specific tryptophan dynamics in the peptide analogues studied here can be discussed in relation to the recently determined x-ray diffraction study of peptide A in fluid multilayers. Hristova et al. (1999) found that a N- and C-terminally-blocked peptide A was located, on average, approximately parallel to the lipid surface with the center of the peptide distribution located near the carbonyl region of the bilayer. Accordingly, the side chains on the polar face of the helix would experience mainly the phosphate headgroups of the phospholipid and water molecules, whereas on the nonpolar face of the helix, the side chains would be closer to the carbonyl groups and hydrocarbon chains of the phospholipid. Thus, suitably exposed tryptophan rotamers at positions 2 and 12 (i.e., on the polar face of the helix) would be expected to exhibit different local rotational dynamics than tryptophans on the nonpolar face (at positions 3, 7, and 14) as a result of differences in microviscosity, hydrogen bonding, and electrostatics. These considerations are in good agreement with our dynamic depolarization measurements of the peptide-lipid complexes. The pattern of limiting anisotropies of the short-correlation time-associated fluorescence (global analysis, Table 2) correlates approximately with the position of the

tryptophan residue relative to the lipid and aqueous phases according to the helical wheel representation shown in Fig. 1. Rotation of the peptide about its long axis on the lipid surface would be energetically unfavorable and, if it occurred, would be severely hindered. The difference in the dynamics of tryptophan side chains on different sides of the helix would, therefore, be preserved. However, this does not preclude the possibility of segmental motions, hindered helix-tilting motions, and rotational precession on the lipid surface in other directions.

With respect to peptide disorder in the direction normal to the bilayer, White and coworkers (Hristova et al., 1999) found that x-ray diffraction data were not compatible with a model in which the peptide helix was parallel to the membrane surface. Other factors, such as helix disorder or helix tilting, were required to fit the observed diffraction data. In terms of the present study, the decrease in the long rotational time constant anisotropy (r_{o2}) as the tryptophan is moved progressively from position 2 to position 14 (Table 2) suggests a gradient of dynamics along the peptide. Such a gradient may arise from a progressive disordering of the helix as the C-terminus is approached, or it may be due to a tilting of the helix such that the microviscosity experienced by a tryptophan rotamer gradually decreases. These observations are in agreement with two x-ray models presented by Hristova et al. (1999) that show backbone dihedral angles dependent on the C_α position in the chain, such that increased fraying of the helix occurs as the C-terminus is approached. Fluctuations of the polypeptide main chain will be partially coupled to the motions of the indole ring and allow free space for indole ring reorientation about the $C_\beta-C_\gamma$ and/or $C_\alpha-C_\beta$ bonds. To make this connection more explicit, we have plotted in Fig. 4 the mean deviation of backbone dihedral angle from the ideal α-helical values for the two x-ray models presented by Hristova et al. (1999) together with the tryptophan dynamic depolarization data for the present peptide-lipid complexes. The dynamic depolarization data are represented in terms of the semi-cone angle for indole ring rotation as formulated in the wobbling-in-cone model (Kinosita et al., 1982; Chang et al., 1988) and calculated from the apparent limiting anisotropy r_{o2} values in Table 2. Although caution must be exercised in directly comparing two quantities which refer to different aspects of the peptide-lipid structure/dynamics, the increase in the level of polypeptide disorder and indole dynamics with sequence position points to the possibility of a motional gradient in the peptide-lipid complexes. Site-specific motional gradients have been observed previously for transmembrane alamethicin analogues measured by tryptophan fluorescence anisotropy decay (Vogel et al., 1988), in helical alanine-based peptides in solution using electron spin resonance spectroscopy (Miick et al., 1993), and in detergent micelle complexes of the fd-coat protein determined with nuclear magnetic resonance spectroscopy (Almeida et al., 1997). The functional significance of a motional gradient in the context of class A helix-lipid interactions is not clear at present but may be important in mediating polypeptide-lipid and helix-helix interactions on lipid surfaces.

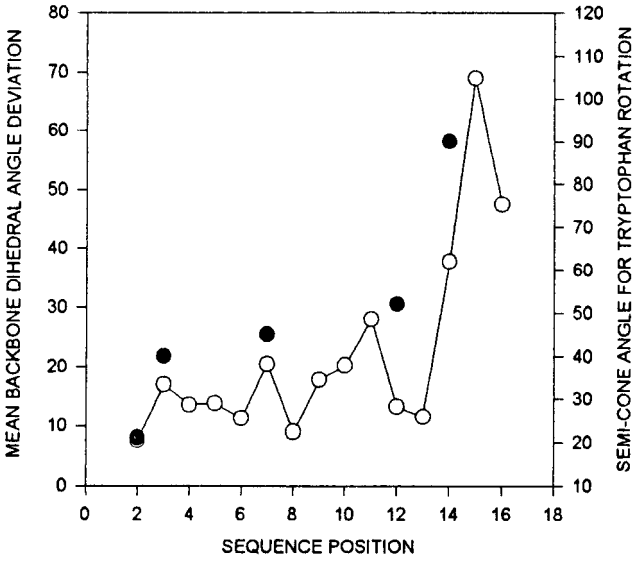

FIGURE 4 Comparison of position dependent polypeptide disorder determined from tryptophan dynamics of the peptide (A-E)-lipid complexes *(filled circles)* and from two disordered helix models determined from x-ray diffraction studies of blocked 18A peptide in phospholipid multilayers *(hollow circles)*. The *filled circles* represent the semi-cone angle for tryptophan rotation derived from the anisotropy decay associated with the long time constant in Table 2 and the wobbling-in-cone model of Kinosita et al. (1982). The *hollow circles* denote the mean deviation of polypeptide backbone dihedral angles from ideal α-helical values for two membrane-incorporated peptide structures proposed by White and coworkers (Hristova et al., 1999).

In summary, dynamic depolarization measurements in the Class A amphipathic peptides studied indicates that the main effect of tryptophan position is not on the magnitude of the correlation times per se but on their associated amplitudes and, therefore, on the degree of restriction of the fluorophore motion. Specifically, the amplitude associated with the short correlation time is affected by the position of the tryptophan on the hydrophilic or hydrophobic side of the helix, whereas that associated with the longer correlation time reflects the position along the sequence. Further work will be required to understand the coupling between the membrane-associated structure and the dynamics of these and related systems.

We acknowledge helpful correspondence with Richard Pastor. The research was supported by the Australian Research Council. A. H. A. C. received partial salary support as an Australian Research Council Postdoctoral Fellow.

REFERENCES

Alcala, J. R. 1995. The effect of harmonic conformational trajectories on protein fluorescence and lifetime distributions. *J. Chem. Phys.* 101: 4578–4584.

Alcala, J. R., E. Gratton, and F. G. Prendergast. 1987. Fluorescence lifetime distributions in proteins. *Biophys. J.* 51:597–604.

Almeida, F. C. L., and S. J. Opella. 1997. fd Coat protein structure in membrane environments:Structural dynamics of the loop between the hydrophobic trans-membrane helix and the amphipathic in-plane helix. *J. Mol. Biol.* 270:481–495.

Beechem, J. M., J. R. Knutson, and L. Brand. 1986. Global analysis of multiple dye fluorescence anisotropy experiments on proteins. *Biochem. Soc. Trans.* 14:832–835.

Belford, G. G., R. L. Belford, and G. Weber. 1972. Dynamics of fluorescence polarization in macromolecules. *Proc. Natl. Acad. Sci. USA.* 69:1392–1393.

Benedetti, E., G. Morelli, G. Nemethy, and H. A. Sheraga. 1983. Statistical and energetic analysis of side-chain conformations in oligopeptides. *Int. J. Peptide. Protein. Res.* 22:1–15.

Chang, M., G. R. Fleming, A. M. Scanu, and N-C. C. Yang. 1988. A high resolution fluorescence decay and depolarization study of human plasma apolipoproteins. *Photchem. Photobiol.* 47:345–355.

Chen, R. F., J. R. Knutson, H. Ziffer, and D. Porter. 1991. Fluorescence of tryptophan dipeptides: Correlations with the rotamer model. *Biochemistry.* 30:5184–5195.

Clayton, A. H. A., and W. H. Sawyer. 1999a. The structure and orientation of class A amphipathic peptides on a phospholipid bilayer surface. *Eur. Biophys. J.* 28:133–141.

Clayton, A. H. A., and W. H. Sawyer. 1999b. Tryptophan rotamer distributions in amphipathic peptides at a lipid surface. *Biophys. J.* 76: 3235–3242.

Clayton, A. H. A., and W. H. Sawyer. 2000. Oriented circular dichroism of a Class A amphipathic helix in aligned phospholipid multilayers. *Biochim. Biophys. Acta.* (In press).

Doring, K., W. Beck, L. Kanermann, and F. Jahnig. 1997. The use of long-lifetime component of tryptophan to detect slow orientation fluctuations of proteins. *Biophys. J.* 72:326–334.

Dornmair, K., and F. Jahnig. 1989. Internal dynamics of lactose permease. *Proc. Natl. Acad. Sci. USA.* 86:9827–9831.

Frey, S., and L. K. Tamm. 1990. Membrane insertion and lateral diffusion of fluorescence-labelled cytochrome c oxidase subunit IV signal peptide in charged and uncharged phospholipid bilayers. *Biochem. J.* 272: 713–719.

Gratton, E., D. M. Jameson, and R. D. Hall. 1984. Multi-frequency phase and modulation fluorometry. *Ann. Rev. Biophys. Bioeng.* 13:105–124.

Hristova, K., W. C. Wimley, V. K. Mishra, G. M. Antharamiah, J. P. Segrest, and S. H. White. 1999. An amphipathic α-helix at a membrane interface: a structural study using a novel x-ray diffraction method. *J. Mol. Biol.* 290:99–117.

John, E., and F. Jahnig. 1988. Dynamics of melittin in water and membranes as determined by fluorescence anisotropy decay. *Biophys. J.* 54:817–827.

Kinosita, K. Jr., A. Ikegami, and S. Kawato. 1982. On the wobbling-in-cone analysis of fluorescence anisotropy decay. *Biophys. J.* 37:461–464.

Knutson, J. R., J. M. Beechem, and L. Brand. 1983. Simultaneous analysis of multiple fluorescence decay curves: a global approach. *Chem. Phys. Lett.* 102:501–507.

Ladokhin, A. S. 1999. Red-edge excitation study of non-exponential fluorescence decay of indole in solution and in a protein. *J. Fluor.* 9:1–9.

Ladokhin, A. S., M. E. Selsted, and S. H. White. 1997. Bilayer interactions of indolicidin, a small antimicrobial peptide rich in tryptophan, proline, and basic amino acids. *Biophys. J.* 72:794–805.

Lakowicz, J. R., G. Laczko, I. Gryczynski, and H. Cherek. 1985. Measurement of subnanosecond anisotropy decays of protein fluorescence using frequency-domain fluorometry. *J. Biol. Chem.* 261:2240–2245.

Maliwal, B. P., A. Hermetter, and J. R. Lakowicz. 1986. A study of protein dynamics from anisotropy decay obtained by variable frequency phase-modulation fluorometry; internal motions of N-methylanthraniloyl melittin. *Biochem. Biophys. Acta.* 873:173–181.

Miick, S. M., K. M. Castel, and G. L. Millhauser. 1993. Experimental molecular dynamics of an alanine-based helical peptide determined by spin label electron spin resonance. *Biochemistry.* 32:8014–802.

Millar, D. P. 1996. Time-resolved fluorescence. *Curr. Opin. Struct. Biol.* 6:637–642.

New, R. R. C. 1990. Preparation of liposomes. *In* Liposomes: A Practical Approach. IRL Press.1–33.

Peng, K., A. J. W. G. Visser, A. van Hoek, C. J. A. M. Wolfs, and M. A. Hemminga. 1990. Analysis of time-resolved fluorescence anisotropy in lipid-protein systems. II Application to tryptophan fluorescence of bacteriophage M13 coat protein incorporated in phospholipid bilayers. *Eur. Biophys. J.* 18:285–293.

Szabo, A. G., and D. M. Rayner. 1980. Fluorescence decay of tryptophan conformers in aqueous solution *J. Am. Chem. Soc.* 102:554–563.

Tieleman, D. P., L. R. Forrest, M. S. P. Sansom, and J. C. Berendsen. 1998. Lipid properties and the orientation of aromatic residues in OmpF, influenza M2 and alamethicin systems: molecular dynamics simulations. *Biochemistry.* 37:17554–17561.

Tirado, M. M., M. C. Lopez Martinez, and G. de la Torre. 1984. Comparison of theories for the translational and rotational diffusion coefficients of rodlike molecules: application to short rodlike cylinders. *J. Chem. Phys.* 81:2047–2052.

Valeur, B., and G. Weber. 1977. Resolution of the fluorescence excitation spectrum of indole into ^1L_a and ^1L_b excitation bands. *Photochem. Photobiol.* 25:441–444.

Vogel, H., L. Nilsson, R. Rigler, K-P. Voges, and G. Jung. 1988. Structural fluctuations of a helical polypeptide traversing a lipid bilayer. *Proc. Natl. Acad. Sci. USA.* 85:5067–5071.